

Shape Optimization of Electrostatically Actuated Micro Cantilever Beam with Extended Travel Range Using Simulated Annealing

R R Trivedi, M M Joglekar, R P Shimpi and D N Pawaskar

Abstract—The pull-in instability places substantial restrictions on the performance of electrostatically driven MEMS devices by limiting their range of travel. Our objective is to present a systematic method of carrying out optimal design of novel types of electrostatic beams that have enhanced travel ranges. In this paper, we implement a shape optimization methodology using simulated annealing to maximize the static pull-in ranges of electrostatically actuated micro-cantilever beams. We use the Rayleigh-Ritz potential energy minimization technique to compute the pull-in displacement and voltage of each micro cantilever beam. A versatile parametric width function is used to characterize non-prismatic micro-cantilever geometries and the pull-in displacement of the cantilever is maximized with respect to the parameters of the proposed width function. Geometric constraints encountered in typical MEMS applications are incorporated into the optimization scheme using a penalty method. The simulated annealing algorithm uses different cooling schedules with the same number of objective function computations. We consider a matrix of several test cases in order to successfully demonstrate the utility of the proposed methodology. Our results indicate that an increase in the pull-in displacement of as much as 20% can be obtained by using our optimization approach. We have also compared our results with those obtained using traditional optimization approaches. We find the results are fairly independent of the cooling schedule used which demonstrates the usefulness and flexibility of this method to carry out optimal design of structural elements under electrostatic loading.

Index Terms—MEMS, Simulated Annealing, Shape Optimization, Pull-in Instability, Electrostatic Actuator, Micro Cantilever

I. INTRODUCTION

THE word MEMS is an acronym for Micro Electro-Mechanical System. Rapidly emerging technology of MEMS combines many diverse fields within engineering and science to develop devices and systems that perform highly precise functions. Successful and commercialized MEMS actuators include digital micro mirror device, automotive crash sensors, ink jet printer nozzles, catheter tip pressure sensors, etc [1]. There are two basic components of MEMS, sensors and actuators. The actuator contains the mechanical members, which are acted upon by various mechanisms like electromagnetic, thermo actuation, use of shape memory alloys, piezo actuation, magneto static actuation and electrostatic actuation. Out of all these, electrostatic actuation is widely used. The popularity of electrostatic actuation in

MEMS is because of their simple construction, compatibility with micro fabrication processes, and lower power consumption relative to other actuation methods [2].

II. BACKGROUND AND MOTIVATION

The principal drawback in using electrostatically driven systems is the well-known pull-in instability in which one of the movable capacitor plates forming the actuator strikes its fixed counterpart after traveling a certain distance. The immediate consequence of pull-in is the snapping of two electrodes, which can cause a short circuit and it will make the device non-functional [3]. Though useful in some of the cases like measurement of the material properties, the inherent phenomenon of pull-in hampers an efficient use of electrostatic actuators in many applications that require greater travel range of operation like digital micro mirror device (DMD) [2],[4]. The origin of the pull-in instability lies in the interaction of nonlinear electrostatic force; which varies as per an inverse square law and the linear mechanical restoring force. Pull-in displacements as percentages of the original gaps in many structural models of these actuators are 33.33% for parallel plates, 45% for cantilevers, 44.04% for torsional actuators and 35.8% for fixed-fixed beams [5]. This means that in most applications more than 50% of the original gap is not available for travel of the movable electrode. This is the motivation behind the present work to propose newer actuators which will permit us to access more of the available gap and will also permit us to gain more control over the pull-in displacement.

Starting from an original prismatic shape (i.e. constant width), the objective of the present work is to arrive at optimum width profiles $b(x)$ for the microcantilever beam such that the occurrence of the pull-in instability is delayed to the maximum possible extent, thereby increasing the travel range of the device [5]. While doing so, we assume a few constraints that are of interest to the engineering design of microbeams. These include, a constant volume constraint and constraints on the maximum and minimum allowable width. The constant volume constraint helps in comparing the two designs (prismatic and nonprismatic), for their performance, when both of them consume same amount of material during their fabrication. In addition, this constraint precludes the role of volume of an actuator in controlling its pull-in parameters and thus allows us to focus on the actuator's shape instead.

The maximum width constraint is motivated from the spatial constraints on the device, such as a fixed number of beam like actuators on a given chip in case of a specific

R R Trivedi M M Joglekar and D N Pawaskar are with the Mechanical Engineering Department, Indian Institute of Technology Bombay, Mumbai 400076 India (e-mail: pawaskar@iitb.ac.in) phone: 91-22-25764558; fax: 91-22-25726875.

R P Shimpi is with the Department of Aerospace Engineering, Indian Institute of Technology Bombay, Mumbai 400076 India.

application. The minimum width constraint is due to the limitation on the minimum feature size that a specific MEMS manufacturing process may have. For example, the design rules of PolyMUMPs suggest the minimum feature size to be limited to 3μ [6]. Also, in some cases, the width of a beam-like structure has to be more than some specific minimum value in order to mount transducer elements on the cantilever [7]. In some configurations, minimum width may be limited by the maximum allowable stress in the microbeam. In this section, we implement the proposed optimization framework to obtain the optimal shapes of electrostatically actuated microbeams which maximize their pull-in range, while obeying the imposed constraints.

To this end, we use simulated annealing as an optimization tool to design electrostatically driven cantilevers with variable geometries that lead to extended travel ranges. There are several other techniques of optimization which can be used for MEMS optimization like Genetic Algorithm and Nelder Mead algorithm [8]. Example of it is GA used for model updating of a multiphysics MEMS Micromirror [9]. Simulated annealing (SA) is one of the most flexible techniques available for solving hard combinatorial problems. The main advantage of SA is that it can be applied to large problems regardless of the conditions of differentiability, continuity, and convexity that are normally required in conventional optimization methods. In this paper, the principles of simulated annealing are presented for MEMS application. As happens with other combinatorial techniques, the coding of solutions, the neighborhood definition of a given configuration, the evaluation function and the transition mechanisms are critical to the success of practical implementations of simulated annealing [10].

In this paper, we use simulated annealing to maximize the static pull-in displacement of a cantilever with respect to design parameters that characterize the in plane geometry of the beam.

III. METHODOLOGY

First we present a Rayleigh-Ritz-based energy minimization method that is used to compute the pull-in parameters (displacement and voltage) of any cantilever beam with variable width [11]. Consider the cantilever beam as shown in figure 1 having length L , width b and thickness h , used as a movable electrode in the electrostatic actuator system. The fixed electrode is located at the bottom and the two electrodes are separated by an initial gap g_0 . When voltage V is applied across the two electrodes, the cantilever deforms under the action of electrostatic force [11].

Using Euler-Bernoulli beam theory, the governing differential equation is given by [12]

$$E \frac{\hat{b}(\hat{x}) h^3}{12} \frac{d^4 \hat{u}(\hat{x})}{d\hat{x}^4} = q(\hat{x}) = \frac{\epsilon \hat{b}(\hat{x}) \hat{V}^2}{(g_0 - \hat{u}(\hat{x}))^2} \quad (1)$$

where, $\hat{u}(\hat{x})$ is the deflection of the beam, which is a function of the coordinate \hat{x} measured along its length. \hat{V} is the applied voltage, ϵ is the permittivity of free space, $\hat{b}(\hat{x})$ is the width at distance \hat{x} from fixed end. Using the appropriate kinematic boundary conditions for the cantilever, the assumed displaced shape can be written in terms of a as

$$\hat{u}(\hat{x}) = a(6L^2 \hat{x}^2 - 4L \hat{x}^3 + \hat{x}^4) \quad (2)$$

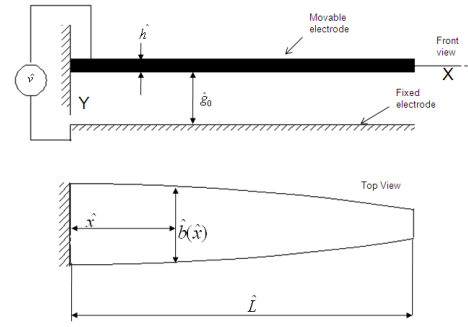


Fig. 1. Schematic of an electrostatically actuated variable width micro cantilever

The total potential energy of the electrostatic-elastic system can be written as

$$\hat{\pi} = \frac{Eh^3}{24} \int_0^L \hat{b}(\hat{x}) \left(\frac{d^2 \hat{u}(\hat{x})}{d\hat{x}^2} \right)^2 d\hat{x} - \frac{\epsilon \hat{V}^2}{2} \int_0^L \frac{\hat{b}(\hat{x}) d\hat{x}}{(g_0 - \hat{u}(\hat{x}))} \quad (3)$$

Assuming the constant width of prismatic beam b_0 , the expression for the $\hat{b}(\hat{x})$ can be written as

$$\hat{b}(\hat{x}) = b_0 \hat{w}(\hat{x}) \quad (4)$$

where \hat{w} represent the scaling of b_0 along the length of the cantilever beam. We now define the following dimensionless entities in order to generalize the analysis.

$$u(x) = \frac{\hat{u}(\hat{x})}{g_0}$$

$$x = \frac{\hat{x}}{L}$$

$$V^2 = \frac{\epsilon b_0 L^4 \hat{V}^2}{2EI g_0^3}$$

$$I = \frac{b_0 h^3}{12}$$

where I is the area moment of inertia of the rectangular prismatic microbeam. Using the above dimensionless entity, the normalized total potential energy can be written as

$$\pi = \frac{12 \hat{\pi} L^3}{E b_0 h^3} \quad (5)$$

Following the principle of minimum potential energy [12] and the condition for instability to determine the pull-in parameters of the system.

$$\frac{d\pi}{da} = 0 \quad (6)$$

$$\frac{Eh^3}{12} \int_0^L b(x) [u''(x)] dx - \frac{\epsilon V^2}{2} \int_0^L \frac{b(x) \frac{du(x)}{da} dx}{[g_0 - u(x)]^2} = 0 \quad (7)$$

$$\frac{d^2 \pi}{da^2} = 0 \quad (8)$$

Numerical integrations in the above equation have been carried out using 9 point Gauss quadrature rule. On simplification, a polynomial equation in a is obtained, which is of 7th order, which also contains the terms of V . If we

assume the values of E, I, ϵ_0, b, L and g_0 as equal to unity for convenience, then the resulting polynomial equation can be solved using voltage iteration scheme. We propose that the variable width along the length of the beam can be described by the function [13]

$$b(x) = \alpha b_0 (1 - fx^n)^m \quad (9)$$

where α, f, m and n are the constants and b_0 is the initial width of a beam and x is the location along the length of the beam.

Our objective is to determine the optimal parameters, α, f, m and n of the width function given by equation 9, which maximize the pull-in displacement. We convert maximization problem into a minimization problem. In the following, we formulate the augmented objective function of optimization using the penalty approach. The optimization problem can be stated as follows

$$\text{Minimize } G(\alpha, m, n, f) = 1 - u_{ps} + P_1(C_{area}) + P_2(C_{b_{min}} + C_{b_{max}} + C_f + C_{mn}) \quad (10)$$

Subject to the following constraints.

$$\frac{b_{min}}{L} \leq \frac{b(x)}{L} \leq \frac{b_{max}}{L} \quad (11)$$

$$\int_0^1 b_0 dx = \int_0^1 b(x) dx \quad (12)$$

$$0 \leq f \leq 1 \quad (13)$$

$$0 \leq m \leq \infty \quad (14)$$

$$0 \leq n \leq \infty \quad (15)$$

where $u_{ps} = u(x)|_{x=1}$, is the maximum deflection of the cantilever beam in static mode. b_{min} is the minimum width and b_{max} is the maximum width allowed in the cantilever beam. P_1 and P_2 are the penalties used on violation of the constraints. The constraints on the minimum and maximum width are driven by the least achievable dimensions in typical MEMS fabrication processes and constraints on dimensions in the end device respectively. The constant area constraint is motivated by the need to avoid trivial solutions of the optimization problem and in addition to observe the effect of shape, rather than the size, on the pull-in behavior of the actuator under considerations [8]. The five constraint related quantities, which are multiplied by the penalties are explained here,

- 1) The term C_{area} quantifies the degree to which the constant-area constraint is violated

$$C_{area} = \left(1 - \int_0^1 b(x) dx\right)^2$$

- 2) The term $C_{b_{min}}$ quantifies the degree to which the minimum width constraint is violated.

$$C_{b_{min}} = [\min(0, b_{min}^i - b_{min})]^2$$

where, b_{min}^i represents the minimum width of the beam-shape that is obtained in any representative intermediate i^{th} iteration.

- 3) The term $C_{b_{max}}$ quantifies the degree to which the constraint on the maximum width is violated. This term is mathematically expressed as,

$$C_{b_{max}} = [\min(0, b_{min}^i - b_{max})]^2$$

where, b_{max}^i represents the maximum width of the beam-shape that is obtained in any representative intermediate i^{th} iteration.

- 4) The value of the parameter f should be between 0 and 1. Zero value of f indicates a prismatic geometry, while $f = 1$ indicates the beam having zero width at the free end, which is practically not possible

$$C_f = [\max(0, (f - 1))]^2 + [\min(0, f)]^2$$

- 5) On similar logic, the indices m and n need to be positive in order to avoid the infeasible geometries of microbeams. This constraint is included in the term C_{mn} , which is mathematically expressed as,

$$C_{mn} = [\min(0, m)]^2 + [\min(0, n)]^2$$

The penalty $P_1 = 100$ is set on the violation of the area constraint. Our numerical experiments have shown that using this value of penalty P_1 , the area constraint is satisfied within 0.025%. The penalty P_2 is set to 10000 in order to strictly satisfy the constraints on the maximum and minimum width and those on the parameters of the width function. As such, it is very difficult to comment on the smoothness of u_{ps} , with respect to the four parameters of the width function, i.e., α, f, m and n . Therefore, instead of numerically calculating the partial derivatives of u_{ps} with respect to the four parameters and then using derivative based algorithms to find their optimal values, it is recommended to use the derivative free algorithms of minimization which operate on the function values rather than their derivatives. The simulated annealing is a well-known random search scheme, originally suggested by S. Kirkpatrick in 1983 [14]. This optimization technique minimizes a scalar-valued nonlinear function of several real variables using only function values, without any derivative information. For the case under investigation, starting from an initial guess of the four parameters α, f, m and n , the SA algorithm modifies the guess in order to reduce the scalar value of G in every iteration. MATLAB programming environment is used to implement the simulated annealing technique of function minimization. In the upcoming section, we present and discuss the results obtained by implementing the proposed optimization framework.

IV. SIMULATED ANNEALING METHODOLOGY

Simulated annealing (SA) is a random-search technique which exploits an analogy between the way in which a metal cools and freezes into a minimum energy crystalline structure (the annealing process) and the search for a minimum in a more general system; it forms the basis of an optimization technique for combinatorial and other problems [15]. The two main features of the simulated annealing process are (1) the transition mechanism between states and (2) the cooling schedule. When applied to combinatorial optimization, simulated annealing aims to find an optimal configuration (or state with minimum energy) of a complex problem. The algorithm employs a random search which not only accepts

changes that decrease the objective function (assuming a minimization problem), but also some changes that increase it [16]. Parameters affecting the result of simulated annealing are initial and final temperature, cooling schedule, number of transitions. Out of these, choice of cooling schedule is most crucial. It is the scheme used for moving from trials at one temperature T_i to another temperature. $T_{i+1} = FT_i$. Here F represents the rate at which cooling is carried out. Procedure to solve optimization problem by SA is as follows [17]

- 1) Let the $f(X)$ is to be minimized for design vector X_i , with the constraints $X_i(l) \leq X_i \leq X_i(u)$
- 2) Start with some initial point X_0 and calculate $f(X_0)$
- 3) At the current state i of the solid with energy $f_i = f(X_0)$ a subsequent set $i + 1$ is generated by applying a perturbation mechanism which transforms the current state into a next state by a small distortion for instance by displacement of a particle. The energy of the next state is f_{i+1} .
- 4) The acceptance of new point $i + 1$ is based on Metropolis criteria
- 5) If $f_{i+1} - f_i \leq 0$, $i + 1$ is accepted as a current state but if $f_{i+1} - f_i > 0$ i is accepted with the probability $P(\Delta f) = e^{-\frac{(f_{i+1} - f_i)}{K_b T}}$
- 6) K_b is a Boltzman constant, T is Temperature $\Delta f = f(X_{i+1}) - f(X_i)$
- 7) Repeat the procedure till T becomes very small

In our application we have used four cooling schedules which are as follows [17]:

- 1) Balling cooling schedule: According to Balling [18]

$$F = \frac{(\log P_s)}{\left(\frac{1}{(N-1)}\right) (\log P_f)} \quad (16)$$

where N = no of iteration, P_s and P_f is the probability of accepting worse move in the beginning and at the respectively.

- 2) Logarithmic cooling schedule:

$$F = \frac{(3\sigma_{old})}{(1 + T_i \log(1 + \delta))} \quad (17)$$

σ_{old} is the standard deviation of the costs of the configurations generated at the previous temperature level i.e. T_i and δ is the distance parameter

- 3) Exponential cooling schedule:

$$F = \frac{1}{e^{(\lambda T_i / \sigma_{old})}} \quad (18)$$

λ is the constant varying from 0.1 to 0.001.

- 4) Geometric cooling schedule: In this schedule F is directly taken in the range from 0.9 to 0.99.

V. RESULTS AND DISCUSSION

In this section, application of simulated annealing optimization technique in obtaining the optimal shapes of micro cantilever beam which maximize their pull-in range is demonstrated. We first consider a matrix of nine test cases formed by three different levels of minimum and maximum width constraints. In order to maintain the generality, we choose $L = 1$. The width of the original prismatic micro cantilever is chosen as $b_0 = 0.15L$ [8]. The three levels of maximum width constraints are chosen as, $b_{max}/L = 0.2, 0.3, 0.4$,

while the three levels of minimum width constraints are chosen as, $b_{min}/L = 0.02, 0.04, 0.06$ as shown in Table I. The present set of nine case is applicable to any beam geometry having the ratio of $\hat{b}_0/\hat{L} = 0.15$. For example for a typical microbeam with length $\hat{L} = 200 \mu\text{m}$ and width $b_0 = 30 \mu\text{m}$, the case with $\hat{b}_{max}/\hat{L} = 0.3$ and $\hat{b}_{min}/\hat{L} = 0.04$ corresponds to the maximum width constraint equal to $60 \mu\text{m}$ and minimum width constraint equal to $8 \mu\text{m}$. For all nine cases, we maximize the travel range by incorporating the procedure mentioned in the previous section. Decreasing the area of overlap between fixed and movable electrode at the weakest section of the beam (free end) reduces the local intensity of the electrostatic force at that location thereby increasing the travel range. Numerical values indicate that for all the nine cases the area constraint is violated by less than 0.025%. Amongst the considered set of nine cases, the travel range can be maximized by 20% using Balling cooling schedule (case 3).

Looking at the result we note that if we give enough time for each cooling schedule the results obtained are very near to those obtained using Nelder Mead algorithm. It is also seen from the results that cases in which narrower at the free end tend to exhibit more travel range. Due to imposed constant-area constraint, more beam material is placed near the fixed end of the micro cantilever beam.

We have used number of iterations $N = 35000$ for all cooling schedules. The width function is as follows

$$b(x) = \alpha b_0 (1 - f(x)^n)^m \quad (19)$$

TABLE I
INPUT DATA FOR VARIOUS CASES

$b_{min}/L \downarrow b_{max}/L \rightarrow$	0.2	0.3	0.4
0.02	Case 1	Case 2	Case 3
0.04	Case 4	Case 5	Case 6
0.06	Case 7	Case 8	Case 9

Initial conditions for all the parameters are as follows. $m = 0$, $n = 1$, $\alpha = 1$, $f = 1$. These values refer to the rectangular geometry.

A. Balling cooling schedule:

Using Balling cooling schedule following are the values of the parameters $P_s = 0.99999$, $P_f = 0.00001$, $T_i = -\frac{1}{(\log P_s)}$.

TABLE II
OPTIMIZED PARAMETERS USING BALLING COOLING SCHEDULE

Case	m	n	α	f	u_{ps}
1	10.250298	4.236121	1.322676	0.19379	0.523135
2	2.578837	1.331798	1.958812	0.617247	0.525621
3	7.668786	1.757603	1.90588	0.289606	0.536894
4	6.890679	9.002083	1.169594	0.306000	0.510665
5	11.584822	1.827703	1.629923	0.144241	0.504795
6	7.639875	1.776813	1.657084	0.212944	0.505416
7	5.853314	3.061333	1.254242	0.174651	0.484518
8	4.310797	3.593793	1.207178	0.224494	0.483571
9	2.55539	1.645953	1.45439	0.397253	0.485762

B. Logarithmic cooling schedule:

Values of the parameters are $T_i = 45800$, $\delta = 0.1$

TABLE III
OPTIMIZED PARAMETERS USING LOGARITHMIC COOLING SCHEDULE

Case	m	n	α	f	u_{ps}
1	7.165915	3.912808	1.337301	0.27012	0.525132
2	5.266267	4.234209	1.327773	0.355997	0.524805
3	4.803242	1.326269	2.108531	0.407502	0.525477
4	2.968883	3.4914	1.26476	0.407891	0.499075
5	7.360817	2.191086	1.50969	0.20894	0.50465
6	7.130526	2.064105	1.542995	0.219369	0.505445
7	5.987075	6.378461	1.109323	0.138207	0.474509
8	1.514529	2.427	1.265898	0.520961	0.482671
9	6.574407	2.457781	1.323455	0.166233	0.486019

C. Exponential cooling schedule:

Using exponential cooling schedule following are the values of the parameters $T_i = 50000$, $\lambda = 0.001$.

TABLE IV
OPTIMIZED PARAMETERS USING EXPONENTIAL COOLING SCHEDULE

Case	m	n	α	f	u_{ps}
1	3.050779	3.626343	1.325517	0.496072	0.516787
2	5.266267	4.234209	1.327773	0.355997	0.524805
3	3.102129	1.710787	1.804173	0.563229	0.533988
4	2.96888	3.4914	1.26476	0.407891	0.49908
5	7.360817	2.191086	1.50969	0.20894	0.50465
6	3.112345	0.870452	2.291207	0.482457	0.497802
7	2.506305	3.821395	1.180953	0.343579	0.481579
8	7.496556	2.103352	1.370872	0.144783	0.483836
9	11.92556	3.139586	1.246247	0.090354	0.484944

D. Geometric cooling schedule:

Using Balling cooling schedule following are the values of the parameters $\alpha = 0.999$, $T_i = 50000$.

TABLE V
OPTIMIZED PARAMETERS USING GEOMETRIC COOLING SCHEDULE

Case	m	n	α	f	u_{ps}
1	2.351767	4.698475	1.229493	0.608871	0.51378
2	12.23655	2.107813	1.743387	0.188148	0.537542
3	2.940951	1.856634	1.724789	0.578311	0.533724
4	15.04048	3.691606	1.276886	0.0909558	0.50161
5	1.993659	1.882712	1.468635	0.554507	0.498626
6	1.87657	2.25872	1.399555	0.584287	0.500995
7	2.506305	3.821395	1.180953	0.343579	0.481579
8	7.358758	2.239256	1.358018	0.153282	0.486289
9	7.358758	2.239256	1.358018	0.153282	0.486289

E. Comparison of Results of SA with Nelder Mead

We have compared the results obtained using various cooling schedule of simulated annealing with the Nelder Mead algorithm for optimization. The percentage of travel range is compared and mentioned in the following table.

TABLE VI
COMPARISON OF TRAVEL RANGE WITH NELDER MEAD ALGORITHM

Case no.	SA Balling	SA Logarithmic	SA Exponential	SA Geometric	Nelder-Mead
1	52.3135	52.5132	51.6787	51.378	52.72
2	52.5621	52.4805	52.4805	53.7542	53.78
3	53.6894	52.5477	53.3988	53.3724	54.06
4	51.0665	49.9075	49.9075	50.161	49.97
5	50.4795	50.465	50.465	49.8626	50.47
6	50.5416	50.5445	49.7802	50.0995	50.48
7	48.4518	47.4509	48.1579	48.1579	48.46
8	48.3571	48.2671	48.3836	48.6289	48.61
9	48.5762	48.6019	48.4944	48.6289	48.61

F. Optimized Shape of the Microcantilever beam

In order to visualize the obtained width profiles, we select representative case(3) and case(7) and plot the optimal shapes of the movable electrode of the cantilever beam in the figures 2 and 3.

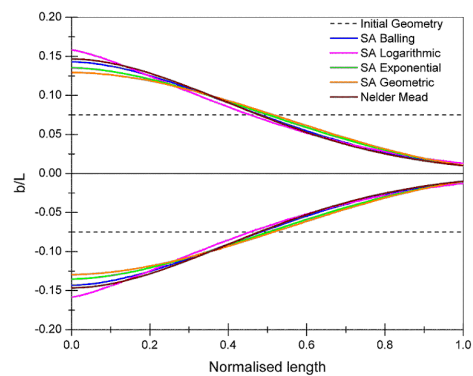


Fig. 2. Optimum width profile for case 3 that result in an enhanced travel range

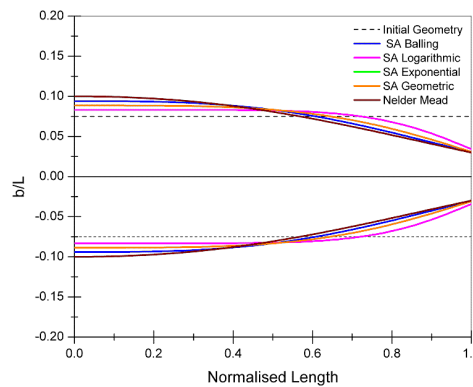


Fig. 3. Optimum width profile for case 7 that result in an enhanced travel range

For a given set of system parameters and constraints, the proposed methodology can thus be applied to obtain the optimum width distribution of micro cantilever beam. In the following we summarize the important conclusions drawn from the investigation.

VI. CONCLUSION

From the above results we can conclude that travel range of cantilever beam under electrostatic loading after optimizing the shape using SA technique can be increased to 53.68% from 45% of the rectangular beam.

If we give large number of iterations for SA almost all the cooling schedules are giving the results very close to each other. But it is difficult to say that whether a particular cooling schedule works better than the rest for all the nine cases. We also compared results obtained from simulated annealing with those obtained using the Nelder-Mead algorithm and find that the two results match reasonably well. In addition, we note that the obtained shapes easily lend themselves to fabrication by surface micromachining techniques and can thus be realized in practice without much difficulty. Based on the case studies in this work, we can conclude that the proposed approach is an effective and flexible design tool capable of solving more complex structural optimization problems encountered in the context of electrostatic actuators

ACKNOWLEDGMENT

The authors would like to gratefully acknowledge financial support from the Industrial Research and Consultancy Center, India Institute of Technology Bombay and the Department of Science and Technology, Government of India.

REFERENCES

- [1] M. Horenstein, S.Pappas, A. Fishov, and T. Bifano, "Electrostatic micromirrors for subaperturing in an adaptive optics system," *Journal of Electrostatics*, vol. 54, pp. 321–332, 2002.
- [2] T.Bifano, J. Perreault, R. Mali, and M. Horenstein, "Microelectromechanical deformable mirrors," *IEEE Journal Of Selected Topics In Quantum Electronics*, vol. 5, no. 1, pp. 83–89, 1999.
- [3] D. Elata, "On the static and dynamic response of electrostatic actuators," *Bulletin Of The Polish Academy Of Sciences*, vol. 53, no. 4, pp. 373–384, 2005.
- [4] M. Hornstein, T.Bifano, S.Pappas, J. Perreault, and R. Mali, "Real time optical correction using electrostatically actuated mems devices," *Journal of Electrostatics*, vol. 46, pp. 91–101, 1999.
- [5] E. Chan and R. Dutton, "Electrostatic micromechanical actuator with extended range of travel," *Journal of Microelectromechanical Systems*, vol. 3, pp. 321–328, 2000.
- [6] D.Koester, A. Cowen, R. Mahadevan, M. Stonefield, and B. Hardy, *PolyMUMPs Design Handbook*. MEMSCAP, 2003.
- [7] H. Fujita and A. Omodaka, "The fabrication of an electrostatic linear actuator by silicon micromachining," *IEEE Transactions on Electron Devices*, vol. 35, no. 6, pp. 731–734, 1988.
- [8] M.Joglekar and D.N.Pawaskar, "Shape optimization of electrostatically actuated microbeams with extended static and dynamic operating ranges," in *Proceed. of ASME 2010 Int. Mech. Engg. Congress Exposition(IMECE 2010-39615)*, pp. 1–10.
- [9] R. J. Link and D. Zimmerman, "An approach for model updating of a multiphysics mems micromirror," *Journal of Dynamic Systems, Measurement and Control*, vol. 129, pp. 357–366, 2001.
- [10] K. Deb, *Optimization for engineering design*. PHI, 2005.
- [11] M. Joglekar, K. Hardikar, and D. Pawaskar, "Analysis of electrostatically actuated narrow microcantilevers using Rayleigh-Ritz energy technique," in *ASME - Int. Conf. Integr. Commer. Micro Nanosystems, MicroNano 2008*, pp. 307–317.
- [12] M. Joglekar and D. N. Pawaskar, "Closed-form empirical relations to predict the static pull-in parameters of electrostatically actuated microcantilevers having linear width variation," *Journal of Microsystem Technol.*, vol. 17, pp. 35–45, 2011.
- [13] M. Joglekar and D.N.Pawaskar, "Estimation of oscillation period/switching time for electrostatically actuated microbeam type switches," *Journal of Mechanical Sciences*, vol. 53, pp. 116–125, 2011.
- [14] S. Kirkpatrick, C. D. Gelatt, and J. M. P. Vecchi, "Optimization by simulated annealing," *Science*, vol. 20, pp. 671–680, 1983.
- [15] E. Aarts and Korst, *Simulated Annealing and Boltzmann Machines*. Chechester: John Wiley, 1989.
- [16] A. Ongkodjojo and F. E. H. Tay, "Global optimization and design for microelectromechanical systems devices based on simulated annealing," *Journal of Micromechanics and microeng.*, vol. 12, no. 117, pp. 878–897, 2002.
- [17] K. Y. Lee and M. E. El-Hawary, *Modern Heuristic Optimization Techniques*. John Wiley and Sons, 2008.
- [18] R.J.Balling, "Optimal steel frame design by simulated annealing," *Journal of structural Engineering*, vol. 6, no. 117, pp. 1780–1795, 1991.